International Journal of Physical Sciences Vol. 7(14), pp. 2145 - 2155, 30 March, 2012
Available online at http://www.academicjournals.org/IJPS
DOI: 10.5897/IJPS11.1039
ISSN 1992 - 1950 ©2012 Academic Journals

Full Length Research Paper

Peristaltic flow of Maxwell fluid in an asymmetric channel with wall properties

S. Hina[1]*, T. Hayat[2], S. Asghar[3] and S. Obaidat[4]

[1]Department of Mathematical Sciences, Fatima Jinnah Women University, Rawalpindi 46000, Pakistan.
[2]Department of Mathematics, Quaid-i-Azam University 45320, Islamabad 44000, Pakistan.
[3]Department of Mathematics, College of Science, King Saud University, P.O.Box 2455, Riyadh 11451, Saudi Arabia.
[4]Department of Mathematics, CIIT, H-8, Islamabad 44000, Pakistan.

Accepted 13 March, 2012

This study is concerned with the peristaltic motion of a Maxwell fluid in an asymmetric compliant channel. The channel asymmetry is created because of peristaltic wave trains of different amplitudes and phases on the channel walls. Mathematical model of the governing problem is first presented and then important phenomenon of "mean flow reversal" is examined. The variations of the interesting parameters entering into the problem are discussed. It was found out that mean velocity in Maxwell fluid is greater than the viscous fluid.

Key words: Maxwell fluid, asymmetric channel, compliant walls.

INTRODUCTION

Peristaltic flows in industry and physiology have generated a lot of interest of the investigators. Specifically, such flows occur in transport of urine from kidney to bladder, chyme movement in the gastrointestinal tract, swallowing of food through the oesophagus, eggs movement in the female fallopian tubes, bile transport in the bile duct, cilia transport and blood circulation in small blood vessels. Finger and roller pumps are designed under the principle of peristaltic transport. In industrial applications, peristaltic flows are useful in sanitary fluid transport, blood pumps in heart lung machine and transport of corrosive fluids. Since the seminal and experimental work of Latham (1966), extensive studies on peristaltic flows have been conducted under different conditions. Majority of the earlier theoretical and experimental studies regarding peristalsis have been reviewed by Jaffrin and Shapiro (1971). Srivastava and Srivastava (1984) reported a summary of most of the theoretical and experimental attempts in view of the geometry, fluid model, Reynolds number, wave number, amplitude ratio, wave shape, etc. Although, relevant literatures on the topic is quite extensive, but few recent investigations can be mentioned by these references (Mekheimer and Elmaboud, 2008a, b; Mekheimer, 2008; Haroun, 2007; Hayat and Ali, 2006; Hayat and Ali, 2008; Hayat et al., 2008a; Elshehawey et al., 2006; Kothandapani and Srinivas, 2008a, b; Hayat and Ali, 2007). Haroun (2006) studied the effect of wall compliance on peristaltic motion of a viscous fluid in an asymmetric channel.

It is accepted now that majority of the biological and industrial fluids are non-Newtonian. Unlike the Newtonian fluids, the non-Newtonian fluids (Vieru et al., 2008a, b; Fetecau and Fetecau, 2006; Tan and Masuoka, 2005a, b; Hayat et al., 2008b, c, d, e, f, g; Wang et al., 2009; Hakeem et al., 2006; Elshahed and Haroun, 2005; Kothandapani and Srinivas, 2008c; Mekheimer et al., 2010) cannot be described by a single constitutive relationship between stress and strain rate. Such constitutive equations give rise to complicated mathematical problems and thus, mathematicians, modelers, physicists and computer scientists encounter wide variety of challenges in constructing analytical and numerical solutions. Generally, the classification of non-Newtonian fluids is based on three categories, namely, the differential

*Corresponding author. E-mail: quaidan85@yahoo.com. Tel: +92 51 90642172. Fax: +92 51 2601171.

type, the rate type and an integral type. Maxwell model is the simplest subclass of rate type fluids. The objective of the present work is to extend the flow analysis of Haroun (2006) from viscous to Maxwell fluid. Series solutions were obtained and discussed.

PROBLEM DEVELOPMENT

We consider an incompressible Maxwell fluid in an asymmetric channel of width $d_1 + d_2$. The channel walls are taken flexible. Furthermore, the sinusoidal travelling waves have been imposed on the compliant walls of channel. Denoting $x-$ and $y-$ components of velocity by u and v, respectively, the continuity and momentum equations are:

$$\frac{\partial u}{\partial x} + \frac{\partial v}{\partial y} = 0, \tag{1}$$

$$\rho \frac{d\mathbf{V}}{dt} = -\nabla p + \operatorname{div} \mathbf{S}, \tag{2}$$

where ρ is the density of fluid, p is the pressure, $\mathbf{V}$ is the velocity field and D/Dt is the upper convective derivative. The constitutive expression for extra stress tensor $\mathbf{S}$ in a Maxwell fluid is:

$$\left(1 + \lambda_1 \frac{D}{Dt}\right)\mathbf{S} = \mu \mathbf{A}_1. \tag{3}$$

In Equation 3, μ is the dynamic viscosity, d/dt is the material derivative, λ_1 is the relaxation time and $\mathbf{A}_1$ is first Rivlin-Ericksen tensor defined as $\mathbf{A}_1 = \operatorname{grad} \mathbf{V} + (\operatorname{grad} \mathbf{V})^T$ and convective derivative of extra stress tensor is defined as:

$$\frac{D\mathbf{S}}{Dt} = \frac{d\mathbf{S}}{dt} - \mathbf{LS} - \mathbf{SL}^T,$$

where $\mathbf{L} = \operatorname{grad} \mathbf{V}$ and $\mathbf{L}^T = (\operatorname{grad} \mathbf{V})^T$.

For two dimensional flow, Equations 2 and 3 give:

$$\rho\left(\frac{\partial u}{\partial t} + u\frac{\partial u}{\partial x} + v\frac{\partial u}{\partial y}\right) = -\frac{\partial p}{\partial x} + \frac{\partial S_{xx}}{\partial x} + \frac{\partial S_{xy}}{\partial y}, \tag{4}$$

$$\rho\left(\frac{\partial v}{\partial t} + u\frac{\partial v}{\partial x} + v\frac{\partial v}{\partial y}\right) = -\frac{\partial p}{\partial y} + \frac{\partial S_{xy}}{\partial x} + \frac{\partial S_{yy}}{\partial y}, \tag{5}$$

$$S_{xx} + \lambda_1\left[\left(\frac{\partial}{\partial t} + u\frac{\partial}{\partial x} + v\frac{\partial}{\partial y}\right)S_{xx} - 2\left(S_{xx}\frac{\partial u}{\partial x} + S_{xy}\frac{\partial u}{\partial y}\right)\right] = 2\mu\frac{\partial u}{\partial x}, \tag{6}$$

$$S_{yy} + \lambda_1\left[\left(\frac{\partial}{\partial t} + u\frac{\partial}{\partial x} + v\frac{\partial}{\partial y}\right)S_{yy} - 2\left(S_{xy}\frac{\partial v}{\partial x} + S_{yy}\frac{\partial v}{\partial y}\right)\right] = 2\mu\frac{\partial v}{\partial y}, \tag{7}$$

$$S_{xy} + \lambda_1\left[\left(\frac{\partial}{\partial t} + u\frac{\partial}{\partial x} + v\frac{\partial}{\partial y}\right)S_{xy} - \left(S_{xx}\frac{\partial v}{\partial x} + S_{yy}\frac{\partial u}{\partial y}\right)\right] = \mu\left(\frac{\partial u}{\partial y} + \frac{\partial v}{\partial x}\right). \tag{8}$$

The compliant wall is constrained to move only in the vertical direction. If η_1 and η_2 are the vertical displacements of the upper and lower walls, then the sinusoidal waves of different amplitudes and phases are given by:

$$\eta_1 = a_1 \cos\frac{2\pi}{\lambda}(x - ct), \qquad \eta_2 = a_2 \cos\left[\frac{2\pi}{\lambda}(x - ct) + \theta\right], \tag{9}$$

in which a_1 and a_2 designate the waves amplitudes, λ is the wavelength, c is the wave speed and $\theta\,(0 \le \theta \le \pi)$ is the phase difference. Note that $\theta = 0$ corresponds to symmetric channel with waves out of phase and for $\theta = \pi$, the waves are in phase. Moreover, $a_1,\ b_1,\ d_1,\ d_2$ and θ obey $a_1^2 + a_2^2 + 2a_1 a_2 \cos\theta \le (d_1 + d_2)^2$. The compliant wall equation is:

$$\left[m\frac{\partial^2}{\partial t^2} + d\frac{\partial}{\partial t} + B\frac{\partial^4}{\partial x^4} - T\frac{\partial^2}{\partial x^2} + K\right]\begin{Bmatrix}\eta_1\\ \eta_2\end{Bmatrix} = p - p_0. \tag{10}$$

where m denotes the plate mass per unit area, d indicates the wall damping coefficient, B is flexural rigidity of the plate, T is the longitudinal tension per unit width, K is the spring stiffness and p_0 is the pressure on the outside surface of the wall. It is assumed that $p_0 = 0$ and the channel walls are inextensible, so the horizontal displacement is assumed zero. Hence, the boundary conditions are expressed by the following equations:

$$\begin{aligned} u &= 0, \quad v = \frac{\partial \eta_1}{\partial t} \quad at \quad y = d_1 + \eta_1, \\ u &= 0, \quad v = -\frac{\partial \eta_2}{\partial t} \quad at \quad y = -d_2 - \eta_2. \end{aligned} \tag{11}$$

By continuity of stresses and same fluid p at $y = d_1 + \eta_1$ and $y = -d_2 - \eta_2$, Equation 4 helps in writing the following equation:

$$\begin{aligned} &\frac{\partial}{\partial x}\left[m\frac{\partial^2}{\partial t^2} + d\frac{\partial}{\partial t} + B\frac{\partial^4}{\partial x^4} - T\frac{\partial^2}{\partial x^2} + K\right]\begin{Bmatrix}\eta_1\\ \eta_2\end{Bmatrix} \\ &= \frac{\partial S_{xx}}{\partial x} + \frac{\partial S_{xy}}{\partial y} - \rho\left(\frac{\partial u}{\partial t} + u\frac{\partial u}{\partial x} + v\frac{\partial u}{\partial y}\right). \end{aligned} \tag{12}$$

The velocity components in terms of stream function ψ can be written as:

$$u=\frac{\partial\psi}{\partial y},\ v=-\frac{\partial\psi}{\partial x}. \tag{13}$$

We define the non-dimensional parameters and variables as:

$$\psi^*=\frac{\psi}{cd_1},\ x^*=\frac{x}{\lambda},\ y^*=\frac{y}{d_1},\ t^*=\frac{ct}{\lambda},\ \eta_1^*=\frac{\eta_1}{d_1},\ \eta_2^*=\frac{\eta_2}{d_1},\ p^*=\frac{d_1^2 p}{c\lambda\mu},$$
$$S_{ij}^*=\frac{d_1 S_{ij}}{c\mu},\ \lambda_1^*=\frac{\lambda_1 c}{d_1},\ m^*=\frac{m}{\rho d_1},\ d^*=\frac{dd_1}{\rho\nu},\ T^*=\frac{Td_1}{\rho\nu^2},\ K^*=\frac{Kd_1^3}{\rho\nu^2},$$
$$B^*=\frac{B}{\rho d_1\nu^2},\ \varepsilon=\frac{a_1}{d_1},\ h=\frac{d_2}{d_1},\ a=\frac{a_2}{a_1},\ \alpha=\frac{2\pi d_1}{\lambda},\ \mathrm{Re}=\frac{cd_1}{\nu},$$

where Re denotes the Reynolds number and α the wave number. After eliminating pressure, the resulting problem in terms of stream function can be expressed as:

$$\frac{\partial}{\partial t}\nabla^2\psi+\psi_y\nabla^2\psi_x-\psi_x\nabla^2\psi_y=\frac{1}{\mathrm{Re}}\left[\frac{\partial^2}{\partial x\partial y}(S_{xx}-S_{yy})+\left(\frac{\partial^2}{\partial y^2}-\frac{\partial^2}{\partial x^2}\right)S_{xy}\right], \tag{14}$$

$$S_{xx}+\lambda_1\left[\left(\frac{\partial}{\partial t}+\psi_y\frac{\partial}{\partial x}-\psi_x\frac{\partial}{\partial y}\right)S_{xx}-2\left(S_{xx}\psi_{xy}+S_{xy}\psi_{yy}\right)\right]=2\psi_{xy}, \tag{15}$$

$$S_{yy}+\lambda_1\left[\left(\frac{\partial}{\partial t}+\psi_y\frac{\partial}{\partial x}-\psi_x\frac{\partial}{\partial y}\right)S_{yy}+2\left(S_{xy}\psi_{xx}+S_{yy}\psi_{xy}\right)\right]=-2\psi_{xy}, \tag{16}$$

$$S_{xy}+\lambda_1\left[\left(\frac{\partial}{\partial t}+\psi_y\frac{\partial}{\partial x}-\psi_x\frac{\partial}{\partial y}\right)S_{xy}-S_{yy}\psi_{yy}+S_{xx}\psi_{xx}\right]=\psi_{yy}-\psi_{xx}, \tag{17}$$

$$\eta_1=\varepsilon\cos\alpha(x-t),\qquad \eta_2=a\varepsilon\cos(\alpha(x-t)+\theta), \tag{18}$$

$$\begin{aligned}&\psi_y=0,\quad \psi_x=-\frac{\partial\eta_1}{\partial t}\quad at\ \ y=1+\eta_1,\\ &\psi_y=0,\quad \psi_x=\frac{\partial\eta_2}{\partial t}\quad at\ \ y=-h-\eta_2,\end{aligned} \tag{19}$$

$$\begin{aligned}&\frac{\partial}{\partial x}\left[m\frac{\partial^2}{\partial t^2}+\frac{d}{\mathrm{Re}}\frac{\partial}{\partial t}+\frac{B}{\mathrm{Re}^2}\frac{\partial^4}{\partial x^4}-\frac{T}{\mathrm{Re}^2}\frac{\partial^2}{\partial x^2}+\frac{K}{\mathrm{Re}^2}\right]\begin{Bmatrix}\eta_1\\ \eta_2\end{Bmatrix}\\ &=\frac{1}{\mathrm{Re}}\left(S_{xx,x}+S_{xy,y}\right)-\left(\psi_{yt}+\psi_y\psi_{xy}-\psi_x\psi_{yy}\right)\ \text{ at } y=\begin{Bmatrix}1+\eta_1\\ -h-\eta_2\end{Bmatrix}.\end{aligned} \tag{20}$$

SOLUTION OF PROBLEM

For series solution, it is reasonable to expand the flow quantities as:

$$\psi = \psi_0 + \varepsilon\psi_1 + \varepsilon^2\psi_2 + ..., \tag{21}$$

$$S_{xx} = S_{xx0} + \varepsilon S_{xx1} + \varepsilon^2 S_{xx2} + ..., \tag{22}$$

$$S_{xy} = S_{xy0} + \varepsilon S_{xy1} + \varepsilon^2 S_{xy2} + ..., \tag{23}$$

$$S_{yy} = S_{yy0} + \varepsilon S_{yy1} + \varepsilon^2 S_{yy2} + ..., \tag{24}$$

$$\left(\frac{\partial p}{\partial x}\right) = \left(\frac{\partial p}{\partial x}\right)_0 + \varepsilon\left(\frac{\partial p}{\partial x}\right)_1 + \varepsilon^2\left(\frac{\partial p}{\partial x}\right)_2 + ... \tag{25}$$

Substituting the aforementioned equations into Equations 14 to 20 and then comparing terms of like powers of ε, we obtain:

$$\frac{\partial}{\partial t}\nabla^2\psi_0 + \psi_{0y}\nabla^2\psi_{0x} - \psi_{0x}\nabla^2\psi_{0y} = \frac{1}{\mathrm{Re}}\left[\frac{\partial^2}{\partial x\partial y}(S_{xx0} - S_{yy0}) + \left(\frac{\partial^2}{\partial y^2} - \frac{\partial^2}{\partial x^2}\right)S_{xy0}\right], \tag{26}$$

$$S_{xx0} + \lambda_1\left[\left(\frac{\partial}{\partial t} + \psi_{0y}\frac{\partial}{\partial x} - \psi_{0x}\frac{\partial}{\partial y}\right)S_{xx0} - 2\left(S_{xx0}\psi_{xy0} + S_{xy0}\psi_{0yy}\right)\right] = 2\psi_{0xy}, \tag{27}$$

$$S_{yy0} + \lambda_1\left[\left(\frac{\partial}{\partial t} + \psi_{0y}\frac{\partial}{\partial x} - \psi_{0x}\frac{\partial}{\partial y}\right)S_{yy0} + 2\left(S_{xy0}\psi_{0xx} + S_{yy0}\psi_{0xy}\right)\right] = -2\psi_{0xy}, \tag{28}$$

$$S_{xy0} + \lambda_1\left[\left(\frac{\partial}{\partial t} + \psi_{0y}\frac{\partial}{\partial x} - \psi_{0x}\frac{\partial}{\partial y}\right)S_{xy0} + S_{xx0}\psi_{0xx} - S_{yy0}\psi_{0yy}\right] = \psi_{0yy} - \psi_{0xx}, \tag{29}$$

$$\begin{aligned} &\psi_{0y}\begin{Bmatrix}1\\-h\end{Bmatrix} = 0, \quad \psi_{0x}\begin{Bmatrix}1\\-h\end{Bmatrix} = 0,\\ &\psi_{0y}\begin{Bmatrix}1\\-h\end{Bmatrix} = 0, \quad \psi_{0x}\begin{Bmatrix}1\\-h\end{Bmatrix} = 0, \end{aligned} \tag{30}$$

$$\frac{1}{\mathrm{Re}}\left(S_{xx0,x} + S_{xy0,y}\right)\begin{Bmatrix}1\\-h\end{Bmatrix} - \left(\psi_{0yt} + \psi_{0y}\psi_{0xy} - \psi_{0x}\psi_{0yy}\right)\begin{Bmatrix}1\\-h\end{Bmatrix} = 0. \tag{31}$$

For steady parallel flow with constant pressure gradient in the $x-$ direction, the result of ψ_0 is:

$$\psi_0 = -K_0\left(hy - \frac{h-1}{2}y^2 - \frac{y^3}{3}\right), \tag{32}$$

$$K_0 = -\frac{\mathrm{Re}}{2}\left(\frac{\partial p}{\partial x}\right)_0.$$

For ε^1 and ε^2 coefficient, the equations are fourth order ordinary differential equations with variable coefficients, All the boundary conditions are not homogeneous. The problems are not eigen values. Therefore, we restrict ourselves to the free-pumping case which means that the fluid is stationary if there is no peristaltic waves. In this case, we put $(\partial p/\partial x)_0 = 0$, that is, $K_0 = 0.$ Now, the first and second order systems were reduced in the following forms:

$$\frac{\partial}{\partial t}\nabla^2\psi_1 = \frac{1}{\mathrm{Re}}\left[\frac{\partial^2}{\partial x\partial y}(S_{xx1} - S_{yy1}) + \left(\frac{\partial^2}{\partial y^2} - \frac{\partial^2}{\partial x^2}\right)S_{xy1}\right], \tag{33}$$

$$S_{xx1} = 2\psi_{1xy},\ S_{yy1} = -2\psi_{1xy},\ S_{xy1} = \psi_{1yy} - \psi_{1xx}, \tag{34}$$

$$\begin{aligned} &\psi_{1y}\begin{Bmatrix}1\\-h\end{Bmatrix} = 0, \quad \psi_{1x}\begin{Bmatrix}1\\-h\end{Bmatrix} = 0,\\ &\psi_{1y}\begin{Bmatrix}1\\-h\end{Bmatrix} = 0, \quad \psi_{1x}\begin{Bmatrix}1\\-h\end{Bmatrix} = 0, \end{aligned} \tag{35}$$

$$\begin{aligned} &\frac{\partial}{\partial x}\left[m\frac{\partial^2}{\partial t^2} + d\frac{\partial}{\partial t} + B\frac{\partial^4}{\partial x^4} - T\frac{\partial^2}{\partial x^2} + K\right]\begin{Bmatrix}\cos\alpha(x-t)\\ a\cos[\alpha(x-t)+\theta]\end{Bmatrix}\\ &= \frac{1}{\mathrm{Re}}\left(S_{xx1,x} + S_{xy1,y}\right)\begin{Bmatrix}1\\-h\end{Bmatrix} - \psi_{1yt}\begin{Bmatrix}1\\-h\end{Bmatrix}, \end{aligned} \tag{36}$$

$$\frac{\partial}{\partial t}\nabla^2\psi_2+\psi_{1y}\nabla^2\psi_{1x}-\psi_{1x}\nabla^2\psi_{1y}=\frac{1}{\mathrm{Re}}\left[\frac{\partial^2}{\partial x\partial y}(S_{xx2}-S_{yy2})+\left(\frac{\partial^2}{\partial y^2}-\frac{\partial^2}{\partial x^2}\right)S_{xy2}\right], \quad (37)$$

$$S_{xx2}+\lambda_1\left[\frac{\partial S_{xx2}}{\partial t}+\left(\psi_{1y}\frac{\partial}{\partial x}-\psi_{1x}\frac{\partial}{\partial y}\right)S_{xx1}-2\left(\psi_{1yy}S_{xy1}+\psi_{1xy}S_{xx1}\right)\right]=2\psi_{2xy}, \quad (38)$$

$$S_{xy2}+\lambda_1\left[\frac{\partial S_{xy2}}{\partial t}+\left(\psi_{1y}\frac{\partial}{\partial x}-\psi_{1x}\frac{\partial}{\partial y}\right)S_{xy1}-\psi_{1yy}S_{yy1}+\psi_{1xx}S_{xx1}\right]=\psi_{2yy}-\psi_{2xx}, \quad (39)$$

$$S_{yy2}+\lambda_1\left[\frac{\partial S_{yy2}}{\partial t}+\left(\psi_{1y}\frac{\partial}{\partial x}-\psi_{1x}\frac{\partial}{\partial y}\right)S_{yy1}+2\left(\psi_{1xy}S_{yy1}+\psi_{1xx}S_{xy1}\right)\right]=-2\psi_{2xy}, \quad (40)$$

$$\begin{aligned}&\psi_{2y}\begin{Bmatrix}1\\-h\end{Bmatrix}\pm\begin{Bmatrix}\cos\alpha(x-t)\\a\cos[\alpha(x-t)+\theta]\end{Bmatrix}\psi_{1yy}\begin{Bmatrix}1\\-h\end{Bmatrix}=0,\\&\psi_{2x}\begin{Bmatrix}1\\-h\end{Bmatrix}\pm\begin{Bmatrix}\cos\alpha(x-t)\\a\cos[\alpha(x-t)+\theta]\end{Bmatrix}\psi_{1yx}\begin{Bmatrix}1\\-h\end{Bmatrix}=0,\end{aligned} \quad (41)$$

$$\begin{bmatrix}\left(S_{xx2,x}+S_{xy2,y}\right)-\mathrm{Re}\,\psi_{2yt}-\mathrm{Re}\left(\psi_{1y}\psi_{1xy}-\psi_{1x}\psi_{1yy}\right)\\\pm\begin{Bmatrix}\cos\alpha(x-t)\\a\cos[\alpha(x-t)+\theta]\end{Bmatrix}\left(S_{xx1,xy}+S_{xy1,yy}-\mathrm{Re}\,\psi_{1yyt}\right)\end{bmatrix}=0,\ \text{at } y=\begin{Bmatrix}1\\-h\end{Bmatrix}. \quad (42)$$

Following a similar procedure as in Equation 15, the differential systems in ψ_1 and ψ_2 are satisfied by:

$$\begin{aligned}\psi_1(x,y,t)&=\frac{1}{2}\left(\phi_1(y)e^{i\alpha(x-t)}+\phi_1^*(y)e^{-i\alpha(x-t)}\right),\\S_{xx1}(x,y,t)&=\frac{1}{2}\left(\phi_2(y)e^{i\alpha(x-t)}+\phi_2^*(y)e^{-i\alpha(x-t)}\right),\\S_{xy1}(x,y,t)&=\frac{1}{2}\left(\phi_3(y)e^{i\alpha(x-t)}+\phi_3^*(y)e^{-i\alpha(x-t)}\right),\\S_{yy1}(x,y,t)&=\frac{1}{2}\left(\phi_4(y)e^{i\alpha(x-t)}+\phi_4^*(y)e^{-i\alpha(x-t)}\right),\end{aligned} \quad (43)$$

$$\begin{aligned}\psi_2(x,y,t)&=\frac{1}{2}\left(\phi_{20}(y)+\phi_{22}(y)e^{2i\alpha(x-t)}+\phi_{22}^*(y)e^{-2i\alpha(x-t)}\right),\\S_{xx2}(x,y,t)&=\frac{1}{2}\left(\phi_{30}(y)+\phi_{33}(y)e^{2i\alpha(x-t)}+\phi_{33}^*(y)e^{-2i\alpha(x-t)}\right),\\S_{xy2}(x,y,t)&=\frac{1}{2}\left(\phi_{40}(y)+\phi_{44}(y)e^{2i\alpha(x-t)}+\phi_{44}^*(y)e^{-2i\alpha(x-t)}\right),\\S_{yy2}(x,y,t)&=\frac{1}{2}\left(\phi_{50}(y)+\phi_{55}(y)e^{2i\alpha(x-t)}+\phi_{55}^*(y)e^{-2i\alpha(x-t)}\right),\end{aligned} \quad (44)$$

in which asterisk denotes the complex conjugate. Now, the second and third sets of differential equations yield:

$$-i\alpha\,\mathrm{Re}\left(\phi_1''-\alpha^2\phi_1\right)=i\alpha\left(\phi_2'-\phi_4'\right)+\left(\phi_3''+\alpha^2\phi_3\right), \quad (45)$$

$$\begin{aligned}&\phi_1'\begin{Bmatrix}1\\-h\end{Bmatrix}=0,\\&\left(\phi_3'+i\alpha\phi_2+i\alpha\,\mathrm{Re}\,\phi_1'\right)\begin{Bmatrix}1\\-h\end{Bmatrix}=\mathrm{Re}\,\delta\begin{Bmatrix}1\\ae^{i\theta}\end{Bmatrix},\end{aligned} \quad (46)$$

$$\delta=-\frac{i\alpha}{\mathrm{Re}}\left(i\alpha\,\mathrm{Re}\,d+m\alpha^2\,\mathrm{Re}^2-\alpha^4B-\alpha^2T-K\right),$$

$$\phi_2=\frac{2i\alpha\phi_1'}{1-i\alpha\lambda_1},\ \phi_3=\frac{\phi_1''+\alpha^2\phi_1}{1-i\alpha\lambda_1},\ \phi_4=\frac{-2i\alpha\phi_1'}{1-i\alpha\lambda_1}. \quad (47)$$

Since our interest is to determine the mean flow rate, therefore, we need $\phi_{20}'(y)$. Hence,

$$\phi_{40}''=\frac{-i\alpha\,\mathrm{Re}}{2}\left(\phi_1\phi_1^{*''}-\phi_1^*\phi_1''\right)', \quad (48)$$

$$\phi_{40} = \phi_{20}^{''} - \frac{i\alpha\lambda_1}{2}\left(\phi_3\phi_1^{*} - \phi_1\phi_3\right)' + \frac{\lambda_1}{2}\left(\phi_4^{*}\phi_1^{''} + \phi_4\phi_1^{*''} + \alpha^2\phi_2\phi_1^{*} + \alpha^2\phi_2^{*}\phi_1\right),$$

$$\phi_{20}^{'}(1) + \frac{1}{2}\left(\phi_1^{*''}(1) + \phi_1^{''}(1)\right) = 0,$$

$$\phi_{20}^{'}(-h) + \frac{1}{2}\left(e^{i\theta}\phi_1^{*''}(-h) + e^{-i\theta}\phi_1^{''}(-h)\right) = 0, \tag{49}$$

$$\begin{bmatrix} \mp\frac{1}{2}\begin{Bmatrix} 1 \\ ae^{i\theta} \end{Bmatrix}\left(\frac{\phi_1^{*''''} + \alpha^2\phi_1^{*''}}{1+i\alpha\lambda_1} - i\alpha\,\mathrm{Re}\,\phi_1^{*''} - i\alpha\phi_2^{*'}\right) \\ \mp\frac{1}{2}\begin{Bmatrix} 1 \\ ae^{-i\theta} \end{Bmatrix}\left(\frac{\phi_1^{''''} + \alpha^2\phi_1^{''}}{1-i\alpha\lambda_1} + i\alpha\,\mathrm{Re}\,\phi_1^{''} + i\alpha\phi_2^{'}\right) \end{bmatrix} \tag{50}$$

$$= \phi_{40}^{'} + \frac{i\alpha\,\mathrm{Re}}{2}\left(\phi_1\phi_1^{*''} - \phi_1^{*}\phi_1^{''}\right), \quad \text{at} \quad y = \begin{Bmatrix} 1 \\ -h \end{Bmatrix}.$$

$$\phi_1(y) = A\cosh(\alpha y) + B\sinh(\alpha y) + C\cosh(\beta y) + D\sinh(\beta y), \tag{51}$$

$$\phi_{20}^{'}(y) = F(y) + g(y) + c_1 y^2 + c_2 y + c_3, \tag{52}$$

$$\beta^2 = \alpha^2(1 - \mathrm{Re}\,\lambda_1) - i\alpha\,\mathrm{Re},$$

$$A = \frac{\delta\left(\cosh(\alpha h) - ae^{i\theta}\cosh\alpha\right)}{i\alpha^2(\sinh\alpha\cosh\alpha h + \cosh\alpha\sinh\alpha h)},$$

$$B = \frac{\delta\left(\sinh(\alpha h) + ae^{i\theta}\sinh\alpha\right)}{i\alpha^2(\sinh\alpha h\cosh\alpha + \cosh\alpha h\sinh\alpha)},$$

The solution of both systems gives:

$$C = -\frac{\alpha\{A(\cosh\beta h\sinh\alpha + \cosh\beta\sinh\alpha h) + B(\cosh\beta h\cosh\alpha - \cosh\beta\cosh\alpha h)\}}{\beta(\sinh\beta h\cosh\beta + \cosh\beta h\sinh\beta)},$$

$$D = \frac{\alpha\{A(\sinh\beta\sinh\alpha h - \sinh\beta h\sinh\alpha) - B(\sinh\beta\cosh\alpha h + \sinh\beta h\cosh\alpha)\}}{\beta(\sinh\beta h\cosh\beta + \cosh\beta h\sinh\beta)},$$

$$c_1 = -\frac{i\alpha^3\,\mathrm{Re}}{4}\left[\left(A - A^{*}\right)\cosh\alpha + \left(B - B^{*}\right)\sinh\alpha\right],$$

$$c_2 = \frac{1}{1+h}\begin{bmatrix} F(-h) + g(-h) + c_1 h^2 - F(1) \\ -g(1) - c_1 - \frac{1}{2}L_1 - \frac{a}{2}L_2 \end{bmatrix},$$

$$c_3 = \frac{1}{1+h}\begin{bmatrix} -F(-h) - g(-h) - c_1 h^2 - hF(1) \\ -hg(1) - c_1 h - \frac{h}{2}L_1 + \frac{a}{2}L_2 \end{bmatrix},$$

$$F(y) = i\alpha\begin{bmatrix} L_3\begin{pmatrix} \left(AC^{*} + BD^{*}\right)\cosh\left(\alpha + \beta^{*}\right)y \\ + \left(AD^{*} + BC^{*}\right)\sinh\left(\alpha + \beta^{*}\right)y \end{pmatrix} \\ + L_4\begin{pmatrix} \left(AC^{*} - BD^{*}\right)\cosh\left(\alpha - \beta^{*}\right)y \\ + \left(BC^{*} - AD^{*}\right)\sinh\left(\alpha - \beta^{*}\right)y \end{pmatrix} \\ + L_5\begin{pmatrix} \left(A^{*}C + B^{*}D\right)\cosh(\alpha + \beta)y \\ + \left(A^{*}D + B^{*}C\right)\sinh(\alpha + \beta)y \end{pmatrix} \\ + L_6\begin{pmatrix} \left(A^{*}C - B^{*}D\right)\cosh(\alpha - \beta)y \\ + \left(B^{*}C - A^{*}D\right)\sinh(\alpha - \beta)y \end{pmatrix} \\ + L_7\begin{pmatrix} \left(CD^{*} + C^{*}D\right)\sinh\left(\beta^{*} + \beta\right)y \\ + \left(CC^{*} + DD^{*}\right)\cosh\left(\beta^{*} + \beta\right)y \end{pmatrix} \\ + L_8\begin{pmatrix} \left(CD^{*} - C^{*}D\right)\sinh\left(\beta^{*} - \beta\right)y \\ + \left(CC^{*} - DD^{*}\right)\cosh\left(\beta^{*} - \beta\right)y \end{pmatrix} \end{bmatrix},$$

$$g(y) = \frac{i\alpha\lambda_1}{2\left(1 + \alpha^2\lambda_1^2\right)}\begin{bmatrix} 2i\alpha^3\lambda_1\left(AA^{*} + BB^{*}\right)\cosh(2\alpha y) + 2i\alpha^3\lambda_1\left(AA^{*} - BB^{*}\right) \\ + 2i\alpha^3\lambda_1\left(AB^{*} + A^{*}B\right)\sinh(2\alpha y) \\ + L_9\left[\left(AC^{*} + BD^{*}\right)\cosh\left(\alpha + \beta^{*}\right)y + \left(AC^{*} - BD^{*}\right)\cosh\left(\alpha - \beta^{*}\right)y\right] \\ + L_9\left[\left(BC^{*} + AD^{*}\right)\sinh\left(\alpha + \beta^{*}\right)y + \left(BC^{*} - AD^{*}\right)\sinh\left(\alpha - \beta^{*}\right)y\right] \\ + L_{10}\left[\left(A^{*}C + B^{*}D\right)\cosh(\alpha + \beta)y + \left(A^{*}C - B^{*}D\right)\cosh(\alpha - \beta)y\right] \\ + L_{10}\left[\left(A^{*}D + B^{*}C\right)\sinh(\alpha + \beta)y + \left(B^{*}C - A^{*}D\right)\sinh(\alpha - \beta)y\right] \\ + L_{11}\left[\left(CC^{*} + D^{*}D\right)\cosh\left(\beta^{*} + \beta\right)y + \left(CC^{*} - D^{*}D\right)\cosh\left(\beta^{*} - \beta\right)y\right] \\ + L_{11}\left[\left(CD^{*} + C^{*}D\right)\sinh\left(\beta^{*} + \beta\right)y + \left(CD^{*} - C^{*}D\right)\sinh\left(\beta^{*} - \beta\right)y\right] \end{bmatrix},$$

$$L_1 = \begin{Bmatrix} \alpha^2\left(A + A^{*}\right)\cosh\alpha + \alpha^2\left(B + B^{*}\right)\sinh\alpha \\ + \beta^{*2}\left(C^{*}\cosh\beta^{*} + D^{*}\sinh\beta^{*}\right) \\ + \beta^2\left(C\cosh\beta + D\sinh\beta\right) \end{Bmatrix},$$

$$L_2 = \begin{Bmatrix} \alpha^2\left(Ae^{-i\theta} + A^{*}e^{i\theta}\right)\cosh\alpha h - \alpha^2\left(Be^{-i\theta} + B^{*}e^{i\theta}\right)\sinh\alpha h \\ + \beta^{*2}e^{i\theta}\left(C^{*}\cosh\beta^{*}h - D^{*}\sinh\beta^{*}h\right) \\ + \beta^2 e^{-i\theta}\left(C\cosh\beta h - D\sinh\beta h\right) \end{Bmatrix},$$

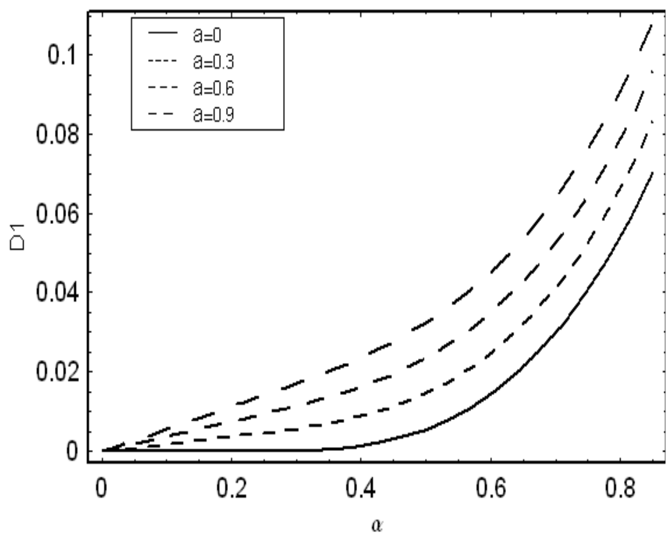

Figure 1. Effect of wave amplitude ratio a on $D1$ versus wave number α when $m=0.01$, $B=20$, $T=10$, $K=10$, $d=0.5$, $h=1$, $R=15$, $\theta=\pi/3$ and $\lambda_1=0.1$.

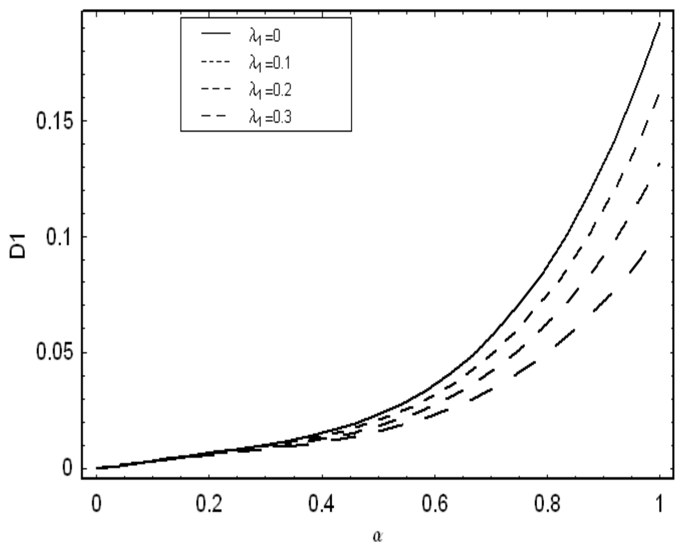

Figure 2. Effect of relaxation parameter λ_1 on $D1$ versus wave number α when $m=0.01$, $B=10$, $T=10$, $K=2$, $h=1$, $R=10$, $\theta=\pi/3$, $a=0.5$ and $d=0.5$.

$$L_3=\left\{-\frac{\mathrm{Re}\left(\beta^{*2}-\alpha^2\right)}{4\left(\alpha+\beta^*\right)^2}+\frac{\alpha\lambda_1\left(\beta^{*2}-\alpha^2\right)}{2\left(\alpha+\beta^*\right)\left(1-i\alpha\lambda_1\right)}\right\},$$

$$L_4=\left\{-\frac{\mathrm{Re}\left(\beta^{*2}-\alpha^2\right)}{4\left(\alpha-\beta^*\right)^2}+\frac{\alpha\lambda_1\left(\beta^{*2}-\alpha^2\right)}{2\left(\alpha-\beta^*\right)\left(1-i\alpha\lambda_1\right)}\right\},$$

$$L_5=\left\{-\frac{\mathrm{Re}\left(\alpha^2-\beta^2\right)}{4\left(\alpha+\beta\right)^2}+\frac{\alpha\lambda_1\left(\alpha^2-\beta^2\right)}{2\left(\alpha+\beta\right)\left(1+i\alpha\lambda_1\right)}\right\},$$

$$L_6=\left\{-\frac{\mathrm{Re}\left(\alpha^2-\beta^2\right)}{4\left(\alpha-\beta\right)^2}+\frac{\alpha\lambda_1\left(\alpha^2-\beta^2\right)}{2\left(\alpha-\beta\right)\left(1+i\alpha\lambda_1\right)}\right\},$$

$$L_7=\left\{-\frac{\mathrm{Re}\left(\beta^{*2}-\beta^2\right)}{4\left(\beta^*+\beta\right)^2}+\frac{\beta\lambda_1\left(\beta^{*2}-\alpha^2\right)}{2\left(\beta^*+\beta\right)\left(1-i\alpha\lambda_1\right)}+\frac{\beta^*\lambda_1\left(\alpha^2-\beta^2\right)}{2\left(\beta^*+\beta\right)\left(1+i\alpha\lambda_1\right)}\right\},$$

$$L_8=\left\{-\frac{\mathrm{Re}\left(\beta^{*2}-\beta^2\right)}{4\left(\beta^*-\beta\right)^2}-\frac{\beta\lambda_1\left(\beta^{*2}-\alpha^2\right)}{2\left(\beta^*-\beta\right)\left(1-i\alpha\lambda_1\right)}+\frac{\beta^*\lambda_1\left(\alpha^2-\beta^2\right)}{2\left(\beta^*-\beta\right)\left(1+i\alpha\lambda_1\right)}\right\},$$

$$L_9=\frac{1}{2}\left[i\alpha\lambda_1\left(3\alpha^2+\beta^{*2}\right)-\left(\beta^{*2}-\alpha^2\right)\right],$$

$$L_{10}=\frac{1}{2}\left[i\alpha\lambda_1\left(3\alpha^2+\beta^2\right)-\left(\alpha^2-\beta^2\right)\right],$$

$$L_{11}=\frac{1}{2}\left[i\alpha\lambda_1\left(2\alpha^2+\beta^2+\beta^{*2}\right)-\left(\beta^{*2}-\beta^2\right)\right].$$

RESULTS AND DISCUSSION

Here, we examine the variations of pertinent parameters occurring in the solution of problem. Emphasis has been given to the mean velocity at the boundaries of the channel, the mean velocity distribution and reversal flow. Figures 1 to 5 indicate the mean velocity at the upper wall that is, $D1$. This axial velocity is related with the mean velocity by $u(1)=\left(\varepsilon^2/2\right)\phi'(1)=\left(\varepsilon^2/2\right)D1$. Figure 1 shows the effects of amplitude ratio a on the mean velocity at the upper wall $D1$ with the wave number α. As expected, $D1$ increases with an increase of a. Figure 2 explains the role of relaxation parameter λ_1 on $D1$ with the wave number α. It is observed that $D1$ is a decreasing function of λ_1. Figure 3 illustrates the influence of $D1$ with the wall elastance K when phase difference has different values. It is noted that $D1$ increases when $0\le\theta\le\pi/2$ and decreases for $\pi/2<\theta\le\pi$. Figure 4 depicts that $D1$ increases with an increase of wall elastance T. However, $D1$ decreases with the increase of Reynolds number Re. Figures 5 and 6 show the behavior of wall damping d and the plate mass per unit area m on $D1$ with Reynolds number Re. These two figures show that $D1$ is a

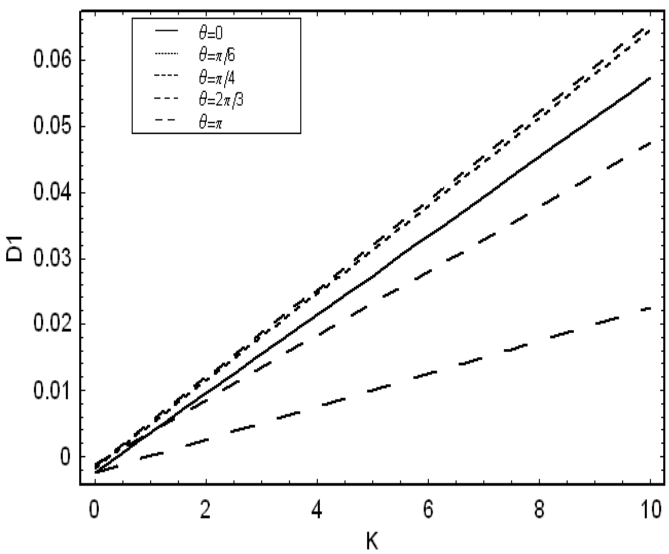

Figure 3. Effect of phase difference θ on $D1$ versus wall elastance K when $m=0.01$, $B=10$, $T=10$, $d=0.2$, $h=1$, $a=0.5$, $\alpha=0.2$, $R=10$ and $\lambda_1=0.1$.

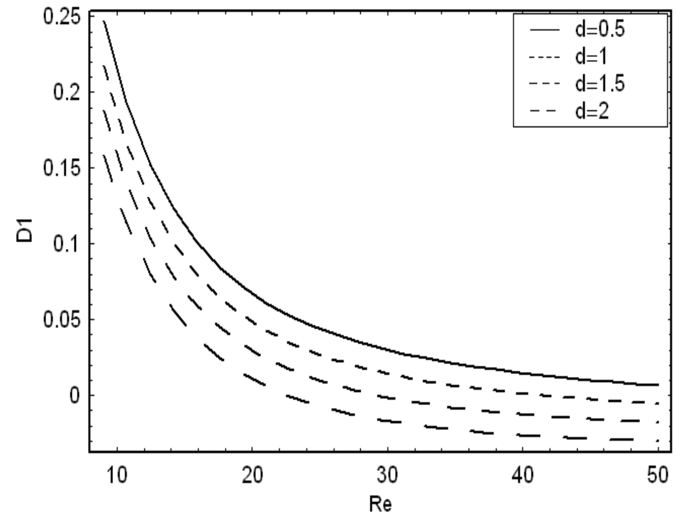

Figure 5. Effect of wall damping d on $D1$ versus Reynolds number Re when $m=0.01$, $B=10$, $K=20$, $T=10$, $a=0.5$, $\alpha=0.4$, $h=1$, $\theta=\pi/6$, $\lambda_1=0.1$.

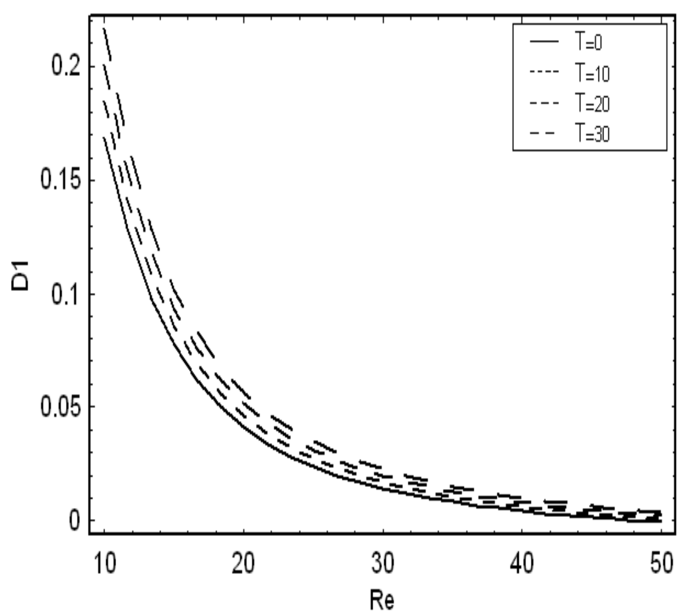

Figure 4. Effect of wall tension T on $D1$ versus Reynolds number Re when $m=0.01$, $B=10$, $K=20$, $d=0.5$, $a=0.5$, $\alpha=0.4$, $h=1$, $\theta=\pi/6$ and $\lambda_1=1$.

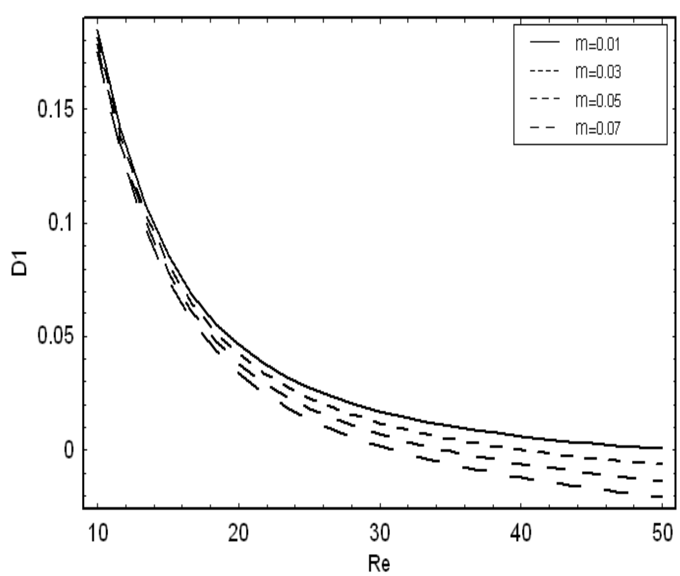

Figure 6. Effect of plate mass per unit area m on $D1$ versus Reynolds number Re when $T=10$, $B=10$, $K=20$, $d=0.5$, $a=0.5$, $\alpha=0.4$, $h=1$, $\theta=\pi/6$ and $\lambda_1=1$.

decreasing function of d and m.

Figures 7 to 13 were plotted to see the effect of wave amplitude a, relaxation parameter λ_1, spring stiffness K, wall elastance T, wall dampind d, plate mass per unit area m and phase difference. It is seen from Figure 7 that the reversal flow decreases when wave amplitude increases. The behavior of relaxation parameter on the mean velocity distribution and the reversal flow is sketched as shown in Figure 8. It is noticed that the reversal flow increases when λ_1 is increased. Figures 9

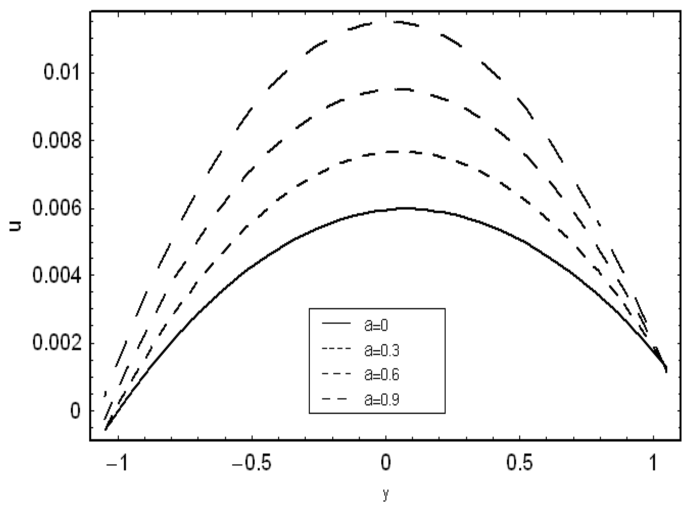

Figure 7. Effect of wave amplitude ratio a on the mean velocity distribution and reversal flow when $m=0.01$, $T=10$, $B=20$, $\mathrm{Re}=70$, $K=50$, $d=0.5$, $\varepsilon=0.5$, $\alpha=0.5$, $h=1$, $\theta=\pi/3$, $\lambda_1=0.1$.

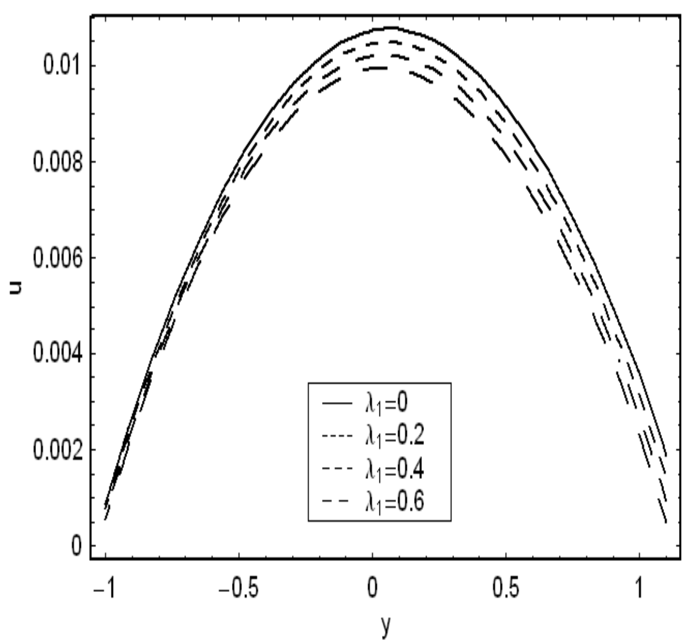

Figure 8. Effect of relaxation parameter λ_1 on the mean velocity distribution and reversal flow when $m=0.01$, $T=10$, $B=20$, $K=40$, $\mathrm{Re}=50$, $d=0.5$, $\varepsilon=0.5$, $\alpha=0.5$, $h=1$, $\theta=\pi/3$ and $a=0.5$.

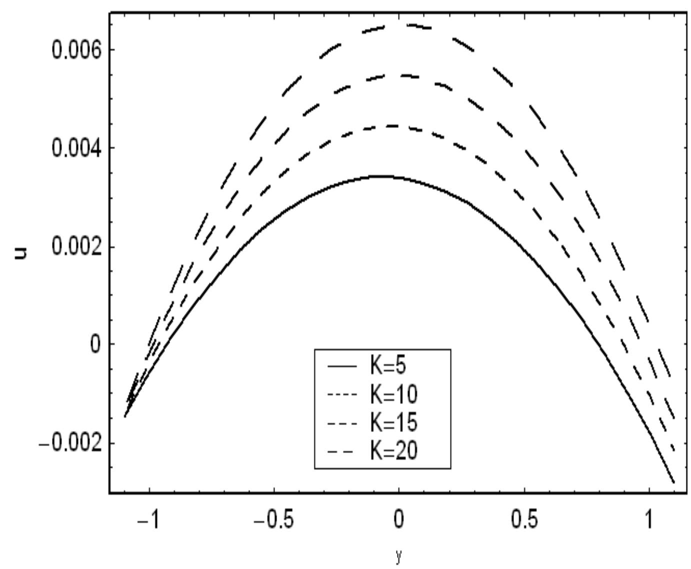

Figure 9. Effect of spring stiffness K on the mean velocity distribution and reversal flow when $m=0.01$, $T=10$, $B=20$, $\mathrm{Re}=50$, $a=0.5$, $d=0.5$, $\varepsilon=0.5$, $\alpha=0.5$, $h=1$, $\theta=\pi/3$ and $\lambda_1=0.1$.

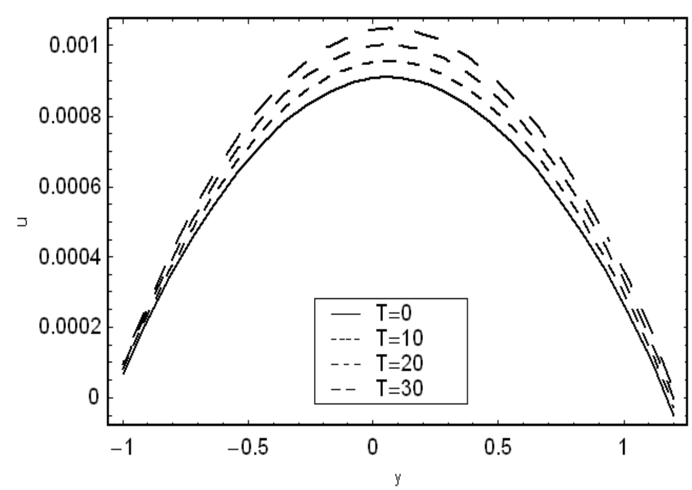

Figure 10. Effect of wall tension T on the mean velocity distribution and reversal flow when $m=0.01$, $B=20$, $\mathrm{Re}=50$, $a=0.5$, $K=40$, $d=0.5$, $\varepsilon=0.15$, $\alpha=0.5$, $h=1$, $\theta=\pi/3$ and $\lambda_1=0.1$.

and 10 elucidate the variation of spring stiffness K and the wall elastance T. The reversal flow decreases when K and T are increased. Figure 11 represents the behavior of wall damping d. This figure depicts that near the boundaries, the reversal flow increases by increasing d while in the remaining wider part of the channel, the flow decreases by increasing d. Figure 12 shows that the reversal flow increases with an increase of

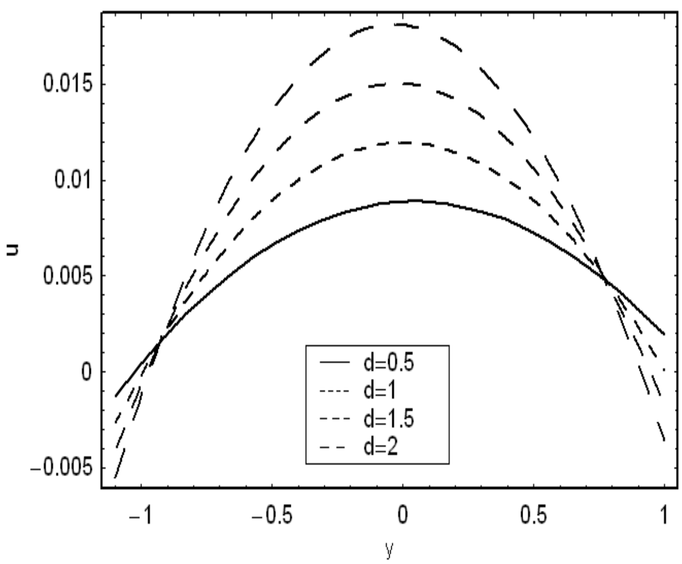

Figure 11. Effect of wall damping d on the mean velocity distribution and reversal flow when $m = 0.01$, $B = 20$, $\mathrm{Re} = 70$, $a = 0.5$, $K = 50$, $T = 10$, $\varepsilon = 0.5$, $\alpha = 0.5$, $h = 1$, $\theta = \pi/3$ and $\lambda_1 = 0.1$.

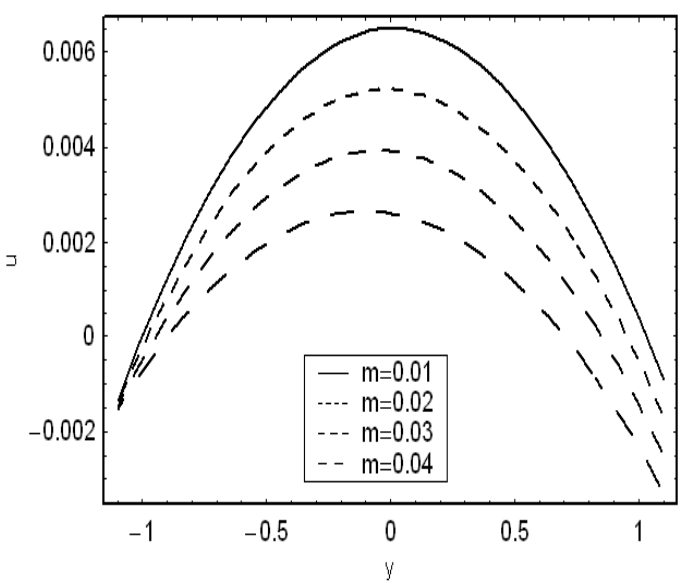

Figure 12. Effect of plate mass per unit area m on the mean velocity distribution and reversal flow when $d = 0.5$, $B = 20$, $\mathrm{Re} = 50$, $a = 0.5$, $K = 20$, $T = 10$, $\varepsilon = 0.5$, $\alpha = 0.5$, $h = 1$, $\theta = \pi/3$ and $\lambda_1 = 0.1$.

plate mass per unit area m. Moreover, the reversal flow decreases with an increase of phase difference when

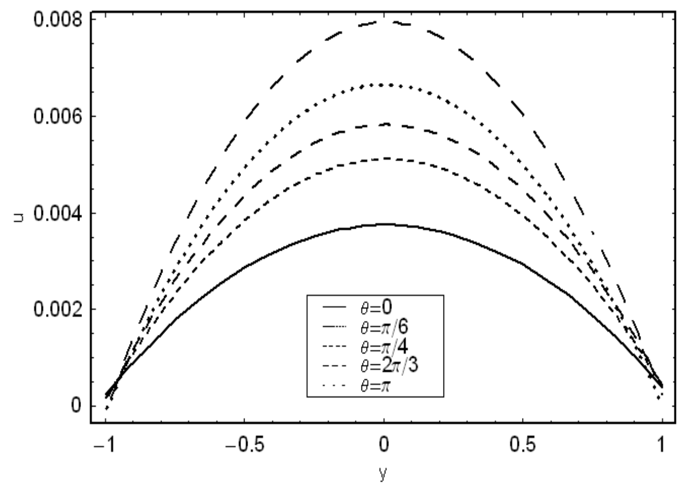

Figure 13. Effect of phase difference θ on the mean velocity distribution and reversal flow when $m = 0.01$, $d = 0.5$, $B = 20$, $\mathrm{Re} = 50$, $a = 0.5$, $K = 20$, $T = 10$, $\varepsilon = 0.5$, $\alpha = 0.5$, $h = 1$ and $\lambda_1 = 0.1$.

$0 \le \theta \le \pi/2$ and increases for $\pi/2 < \theta \le \pi$ (Figure 13).

ACKNOWLEDGEMENTS

The authors thank the Global Research Network for Computational Mathematics and King Saud University, Saudi Arabia for their support.

REFERENCES

Elshahed M, Haroun MH (2005). Peristaltic transport of Johnson-Segalman fluid under effect of a magnetic field. Math. Prob. Eng., 6: 663-667.

Elshehawey EF, Eldabe NT, Elghazy EM, Ebaid A (2006). Peristaltic transport in an asymmetric channel through a porous medium, Appl. Math. Comut., 182: 140-150.

Fetecau C, Fetecau C (2006). Starting solutions for the motion of a second grade fluid due to longitudinal and torsional oscillations of a circular cylinder, Int. J. Eng. Sci., 44: 788-796.

Hakeem AE, Naby AE, Misery AEME, Kareem FMAE (2006). Effects of magnetic field on trapping through peristaltic motion for generalized Newtonian fluid in channel. Physica A, 367: 79-92.

Haroun MH (2006). Effect of wall compliance on peristaltic transport of a Newtonian fluid in an asymmetric channel. Math. Prob. Eng., 61475: (1-19).

Haroun MH (2007). Effect of Deborah number and phase difference on peristaltic transport of a third grade fluid in an asymmetric channel. Comm, Non-Linear Sci. Numer. Simul., 12: 1464-1480.

Hayat T, Afsar A, Ali N (2008c). Peristaltic transport of a Johnson--Segalman fluid in an asymmetric channel, Math. Comp. Model, 47: 380-400.

Hayat T, Ahmad N, Ali N (2008f). Effects of an endoscope and magnetic field on the peristalsis involving Jeffery fluid, Comm. Nonlinear Sci. Numer. Simul., 13: 1581-1591.

Hayat T, Ali N (2006). Peristaltically induced motion of a MHD third

grade fluid in a deformable tube, Phys. A, 370: 225-239.
Hayat T, Ali N (2007). Peristaltic motion of a Carreau fluid in an asymmetic channel, Appl. Math. Comut., 193: 535-552.
Hayat T, Ali N (2008). Effects of an endoscope on the peristaltic flow of a micropolar fluid, Math. Comp. Model, 48: 721-733.
Hayat T, Alvi N, Ali N (2008g). Peristaltic mechanism of a Maxwell fluid in an asymmetric channel. Nonlinear Analysis, Real World Applica, 9: 1474-1490.
Hayat T, Fetecau C, Abbas Z, Ali N (2008e). Flow of Maxwell fluid between two side walls due to a suddenly moved plate. Nonlinear Analysis, Real World Applica., 9: 2288-2295.
Hayat T, Hussain Q, Ali N (2008d). Influence of partial slip on the peristaltic flow in a porous medium. Phys A, 387: 3399-3409.
Hayat T, Javed M, Asghar S (2008b). MHD peristaltic motion of Johnson-Segalman fluid in a channel with compliant walls, Phys. Lett. A, 372: 5026-5036.
Hayat T, Qureshi MU, Ali N (2008a). The influence of slip on the peristaltic motion of a third order fluid in an asymmetric channel, Phys. Lett. A, 372: 2653-2664.
Jaffrin MY, Shapiro AH (1971). Peristaltic pumping, Ann. Review Fluid. Mech., 3: 13-16.
Kothandapani M, Srinivas S (2008a). Nonlinear peristaltic transport of a Newtonian fluid in an inclined asymmetric channel through a porous medium, Phys. Lett. A, 372: 1265-1276.
Kothandapani M, Srinivas S (2008b). On the influence of wall properties in the MHD peristaltic transport with heat transfer and porous medium, Phys. Lett. A, 372: 4586-4591.
Kothandapani M, Srinivas S (2008c). Peristaltic transport of a Jeffrey fluid under the effect of magnetic field in an asymmetric channel, Int. J. Nonlinear Mech., 43: 915-924.
Latham TW (1966). Fluid motion in a peristaltic pump. MS Thesis, MIT Cambridge MA.
Mekheimer KS (2008). Effect of induced magnetic field on peristatic flow of a couple stress fluid. Phys. Lett. A, 372: 4271-4278.
Mekheimer KS, Elmaboud YA (2008a). The influence of heat transfer and magnetic field on peristaltic transport of a Newtonian fluid in a vertical annulus: Application of an endoscope, Phys. Lett., A 372: 1657-1665.
Mekheimer KS, Elmaboud YA (2008b). Peristaltic flow of a couple stress fluid in an annulus: Application of an endoscope, Phys. Lett. A, 387: 2403-2415.
Mekheimer KS, Husseny SZA, Elmaboud YA (2010). Effect of heat transfer and space porosity on peristaltic flow in a vertical asymmetric channel, Numer. Methods Partial Diff. Eqs., 26: 747-770.
Srivastava LM, Srivastava VP (1984). Peristaltic transport of blood: Casson model 2. J. Biomech., 17: 821-829.
Tan WC, Masuoka T (2005a). Stoke's first problem for second grade fluid in a porous half space with heated boundary, Int. J. Nonlinear Mech., 40: 515-522.
Tan WC, Masuoka T (2005b). Stoke's first problem for an Oldroyd-B fluid in a porous half space, Phys. Fluid, 17: 023101-023107.
Vieru D, Fetecau C, Fetecau C (2008a). Flow of viscoelastic fluid with the frictional Maxwell model between two side walls perpendicular to a plate, Appl. Math. Comput., 200: 459-464.
Vieru D, Nazar M, Fetecau C, Fetecau C (2008b). New exact solutions corresponding to the first problem of Stokes for Oldroyd-B fluid, Comp. Maths. Appl., 55: 1644-1652.
Wang Y, Ali N, Hayat T, Oberlack M (2009). Slip effects on the peristaltic flow of a third grade fluid in circular cylinder, ASME J. Appl. Mech., 76: 011006100-011006110.